NASA TECHNICAL NOTE

NASA TN D-2365

C.1

NASA TN D-2365

ANALYSIS OF NON-LINEAR NOISE IN FDM TELEPHONY TRANSMISSION OVER AN SSB-PM SATELLITE COMMUNICATION SYSTEM

by Paul J. Heffernan

Goddard Space Flight Center
Greenbelt, Md.

NATIONAL AERONAUTICS AND SPACE ADMINISTRATION • WASHINGTON, D. C. • JULY 1964

ANALYSIS OF NON-LINEAR NOISE IN FDM TELEPHONY TRANSMISSION OVER AN SSB-PM SATELLITE COMMUNICATION SYSTEM

By Paul J. Heffernan

Goddard Space Flight Center
Greenbelt, Md.

NATIONAL AERONAUTICS AND SPACE ADMINISTRATION

For sale by the Office of Technical Services, Department of Commerce,
Washington, D.C. 20230 -- Price $1.00

ANALYSIS OF NON-LINEAR NOISE IN FDM TELEPHONY TRANSMISSION OVER AN SSB-PM SATELLITE COMMUNICATION SYSTEM

by

Paul J. Heffernan

Goddard Space Flight Center

SUMMARY

Under high received signal conditions, voice channel quality in FDM telephony transmission over an SSB-PM satellite communication system is limited by dynamic non-linearity and down-link differential group delay. This report analyzes the noise produced by dynamic non-linearity in elements of the SSB up-link, spacecraft phase modulator, and ground receiver demodulator. Worst-case channel signal-to-non-linear-noise power ratios are developed in terms of the coefficients of a power series expressing the non-linear characteristic. The group delay problem is not treated. Four appendixes discuss in detail the calculation of the autocorrelation function, the evaluation of spectral convolutions, the determination of the power series coefficients, and CCIR terminology and multichannel loading procedures for FDM telephony.

CONTENTS

ANALYSIS OF NON-LINEAR NOISE IN FDM TELEPHONY TRANSMISSION OVER AN SSB-PM SATELLITE COMMUNICATION SYSTEM

by
Paul J. Heffernan
Goddard Space Flight Center

INTRODUCTION

This report analyzes the effects of certain non-linearities in the transmission of frequency-division-multiplex (FDM) telephony over an SSB-PM communication link of the advanced Syncom* type.

Voice channel quality in an FDM SSB-PM link is determined by two factors: thermal noise, and intermodulation or non-linear noise. Non-linear noise is the unintelligible crosstalk in a voice channel due to the harmonics and intermodulations of the complex multichannel signal generated by system non-linearities. It resembles thermal noise to the ear but, unlike thermal noise, vanishes when the multichannel signal is removed.

With a weak received signal, thermal noise usually limits channel quality. However, with a strong received signal, thermal noise may be insignificant as compared with the non-linear noise; and in this case system non-linearities limit the channel quality. Under certain conditions, system parameters can be optimized by trading one type of interference for the other.

There are two important sources of non-linear noise in an SSB-PM system: dynamic non-linearities and down link differential group delay. Dynamic non-linearities are encountered in the amplitude characteristics of base-band multichannel amplifiers, klystrons, and phase modulators and discriminators.

Differential group delay is encountered on the down link when the instantaneous phase deviation $\phi(t)$ of the modulated carrier is modified non-linearly by a passive selective circuit as a function of the instantaneous frequency $\dot{\phi}(t)$.

This paper analyzes the effects of dynamic non-linearities in detail, and does not treat the group delay problem.

The principle source of non-linear noise in the SSB up-link is the dynamic characteristic of the ground transmitter power amplifier. Multichannel telephony has a peak-to-average ratio of

*Synchronous Communications Satellite.

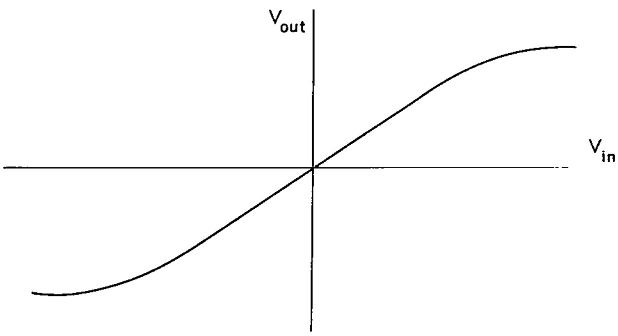

Figure 1—Typical dynamic characteristic of a klystron power amplifier.

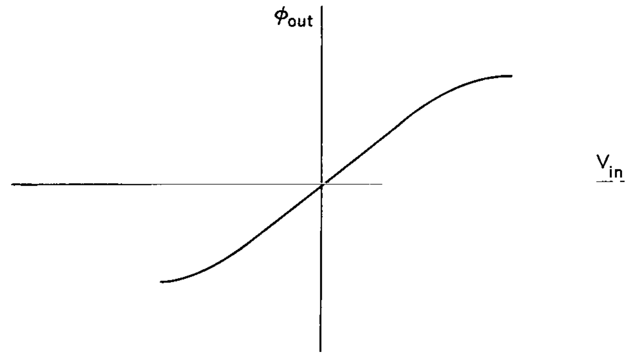

Figure 2—Non-linear characteristic of a phase modulator.

approximately 13 db (Reference 1). Hence, the ground transmitter power amplifier must be linear over a considerable dynamic range, and in general is required to operate well below saturation.

In the spacecraft, all converters and amplifiers prior to the phase modulator must be dynamically linear. Because of the multiple access consideration, these units must be designed for considerably greater dynamic ranges than must the ground transmitter; thus linearity may be a problem despite the low levels at which these units operate.

In the PM down link, non-linearities in the characteristics of the spacecraft phase modulator and ground receiver demodulator introduce non-linear noise in exactly the same manner as do dynamic non-linearities in the up-link.

The CCIR recommends (Reference 2) that for purposes of analysis and testing, a multichannel telephony signal may be represented by a band of white Gaussian noise. Hence, either the instantaneous amplitude of the multichannel signal (on the SSB up-link) or the instantaneous phase deviation of the modulated carrier (on the PM down-link) may be represented by a real stationary random variable $x(t)$ of Gaussian statistics and narrowband white spectral density.

Where the non-linear characteristic of an element can be expressed as a power series of the input $x(t)$, the output ratio of channel test-tone power to the weighted non-linear noise power produced by the element can be computed in terms of the power series coefficients and the variance of $x(t)$. For a system of N channels, CCIR multichannel loading factors relate the mean square value of $x(t)$ to the power or mean square phase deviation corresponding to channel test-tone.

Hence, the performance of a non-linear element in the SSB-PM link can be specified in terms of its power series coefficients and how hard it is driven by a standard signal.

DESCRIPTION OF METHOD

In the time domain, the output $y(t)$ of a zero-memory non-linear device may be generally expressed as a power series of the input $x(t)$;

$$y(t) = \alpha x(t) + \beta x^2(t) + \gamma x^3(t) + \delta x^4(t) + \cdots$$

For systems and devices which are essentially linear, and only deviations from linearity are being considered, the power series converges rapidly, and terms higher than the cubic may ordinarily be ignored. Where basically non-linear devices (rectifiers or limiters) are being treated, higher order terms must be included for an accurate representation.

In the frequency domain, the power spectrum of the output $y(t)$ may quite generally be obtained from a knowledge of $x(t)$ and the coefficients α, β, γ etc.

For the present case where $x(t)$ is a stationary random variable, the power spectrum of $y(t)$ can be calculated by using the Wiener-Khinchin theorem and the statistical properties of $x(t)$ (probability density function, autocorrelation function, spectral density, etc.)

The Wiener-Khinchin theorem states that the autocorrelation function of a sample function of a random process and the spectral density of the process form a Fourier transform pair. If $x(t)$ is a real sample function of a stationary random process, we have that its autocorrelation function is defined as

$$R_x(\tau) = \lim_{T\to\infty} \frac{1}{2T} \int_{-T}^{T} x(t)\, x(t+\tau)\, dt = \overline{x(t)\, x(t+\tau)}$$

and is independent of time.

The theorem states that

$$S_x(f) = \mathcal{F}\left[R_x(\tau)\right]$$

$$R_x(\tau) = \mathcal{F}^{-1}\left[S_x(f)\right]$$

where $S_x(f)$ is the spectral density of the random process.

If $x(t)$ is the input to a non-linear device with output $y(t)$, we have the output autocorrelation function

$$R_y(\tau) = \overline{y(t)\, y(t+\tau)} \quad ;$$

and we can operate on this to get the spectral density $G_y(f)$ of $y(t)$:

$$G_y(f) = \mathcal{F}\left[R_y(\tau)\right]$$

This method of determining the output spectrum of a non-linear device is quite general and very powerful.

For FDM telephony a knowledge of the output spectrum permits the determination of channel signal-to-noise ratios directly. The method used here may be considered an analytical equivalent of the noise-loading procedures widely used to test FDM equipment and systems (Reference 3).

The heart of the problem is to determine the output autocorrelation function $R_y(\tau)$. This demands thorough knowledge of the statistics of the input $x(t)$ and the power series coefficients. It is possible, but not always desirable, to develop a closed form expression for $R_y(\tau)$. For the power series case with Gaussian statistics, we can calculate $R_y(\tau)$ in terms of a power series in $R_x(\tau)$, considerably simplifying the mathematics.

CALCULATION OF OUTPUT SPECTRA AND S/N RATIOS

The input to the non-linear element of the SSB-PM system is a stationary Gaussian functional of zero mean and variance $\overline{x^2}$; i.e., we have

$$p(x) = \frac{e^{-x^2/2\sigma^2}}{\sqrt{2\pi\sigma^2}} ,$$

$$\overline{x} = 0 ,$$

$$\overline{x^2} = \sigma^2 .$$

The autocorrelation function is

$$R_x(\tau) = \overline{x(t)\, x(t+\tau)}$$

and

$$R_x(0) = \overline{x^2(t)} = \overline{x^2(t+\tau)} = \sigma^2$$

The spectral density $S_x(f)$ of the multichannel signal is defined as the average power per unit bandwidth and is an even (two-sided) function of frequency.

From the Wiener-Khinchin theorem,

$$S_x(f) = \int_{-\infty}^{\infty} R_x(\tau)\, e^{-j\omega\tau}\, d\tau$$

and

$$R_x(\tau) = \int_{-\infty}^{\infty} S_x(f)\, e^{j\omega\tau}\, df$$

Assuming a converging power series expresses the non-linear characteristic, the output is

$$y(t) = \alpha x(t) + \beta x^2(t) + \gamma x^3(t) + \delta x^4(t) + \cdots$$

The output autocorrelation function is

$$R_y(\tau) = \overline{y(t)\,y(t+\tau)}$$

Truncating the power series, we have

$$y(t)\,y(t+\tau) = \left[\alpha x(t) + \beta x^2(t) + \gamma x^3(t)\right] \cdot \left[\alpha x(t+\tau) + \beta x^2(t+\tau) + \gamma x^3(t+\tau)\right]$$

and $R_y(\tau)$ will be the sum of the expectations of each of the terms produced in the multiplication. It is at this point that the statistics of $x(t)$ enter the analysis. For $x(t)$ a Gaussian functional of zero mean and variance $\overline{x^2}$, the autocorrelation function (Appendix A) is

$$\begin{aligned} R_y(\tau) &= \beta^2\,\overline{x^2} \\ &+ \left[\alpha^2 + 6\alpha\gamma\,\overline{x^2} + 9\gamma^2\left(\overline{x^2}\right)^2\right] R_x(\tau) \\ &+ \left[2\beta^2 + 24\beta\gamma\,\overline{x^2}\right] R_x^2(\tau) \\ &+ \left[6\gamma^2\right] R_x^3(\tau) \quad . \end{aligned}$$

The power spectrum $G_y(f)$ of the output $y(t)$ can now be obtained by forming the Fourier transform of the entire expression.

The first term represents dc energy, since the transform of a constant in the time domain is a delta function at zero frequency:

$$\int_{-\infty}^{\infty} k e^{-j\omega\tau}\, d\tau = k \lim_{T\to\infty} \left(\frac{\sin 2\pi f T}{\pi f}\right) = k\delta(f) \quad .$$

For the purpose of computing the output spectrum, this term can be ignored.

The terms in the coefficients of $R_x(\tau)$ and $R_x^2(\tau)$ proportional to $\overline{x^2}$ represent second order effects which may be disregarded for the purpose of computing the output spectrum.* The

*This is so if the power series for y(t) converges rapidly. However, terms like $6\alpha\gamma \overline{x^2}$ are interesting in their own right. They indicate that the apparent linear gain of the non-linear element depends on the variance of the Gaussian input. Lewin (Reference 4) has shown the instantaneous waveforms corresponding to these spectral terms are always in exact phase coherence with the freely transmitted waveform. Hence, these can hardly be called distortion spectra. For a single tone input, terms of this type mathematically represent the action of a tuned limiter, and provide a convenient means of determining the power series coefficients α, β, γ, etc., of a non-linear element (see Appendix B).

autocorrelation function is then written

$$R_y(\tau) \approx \alpha^2 R_x(\tau) + 2\beta^2 R_x^2(\tau) + 6\gamma^2 R_x^3(\tau) .$$

The first term is transformed to yield a first order spectrum $G_1(f)$ of the freely transmitted signal.

$$G_1(f) = \int_{-\infty}^{\infty} \alpha^2 R_x(\tau) e^{-j\omega\tau} d\tau = \alpha^2 S_x(f) .$$

Note that the effect is simply that of a linear bandpass filter of gain α.

The other terms yield second, third, and fourth order spectra proportional to convolutions of the input spectrum $S_x(f)$ with itself.

$$G_2(f) = 2\beta^2 S_x(f) * S_x(f) ,$$

$$G_3(f) = 6\gamma^2 S_x(f) * S_x(f) * S_x(f) .$$

These convolutions are evaluated in Appendix C.

It may be seen that the output signal to non-linear noise power ratio at any frequency is given by

$$\frac{P_s}{P_n} = \frac{G_1(f)}{G_2(f) + G_3(f)} .$$

To evaluate the spectral convolutions, it is necessary at this point to define more completely the input spectral density $S_x(f)$ for the two situations of interest in this analysis, i.e., multichannel telephony spectra at baseband and IF. Figure 3 shows these two cases.

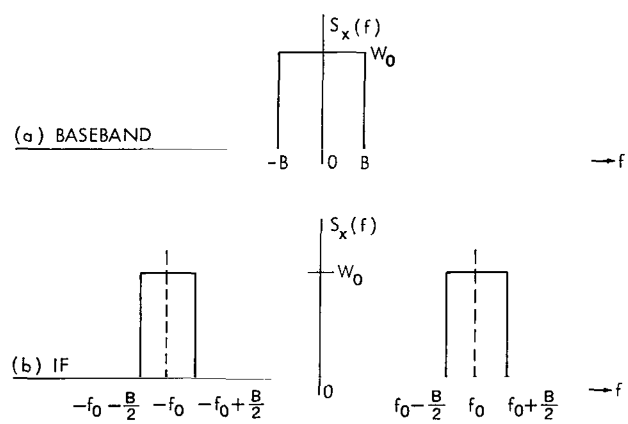

Figure 3—Multichannel signal spectra at baseband and IF.

In either case, the spectral density is the average power per unit bandwidth, and has the value

$$W_0 = \frac{\overline{x^2}}{2B}$$

within the band and is zero outside the band. Spectral density is an even function of frequency

$$S_x(f) = S_x(-f) ,$$

and we have that

$$\int_{-\infty}^{\infty} S_x(f)\,df = \overline{x^2} .$$

Baseband Case

The spectrum of the multichannel signal at baseband is shown in Figure 3(a). In reality, the spectrum does not extend to zero frequency; but for the purpose of this report no significant error is introduced by this representation, since dc levels produced by system non-linearities are filtered out by the natural system bandwidth limitations and need not be considered.

The convolutions $S_x(f)*S_x(f)$ and $S_x(f)*S_x(f)*S_x(f)$ for the baseband case are evaluated in Appendix C and shown in Figure C7. The baseband non-linear noise spectra $G_2(f)$ and $G_3(f)$ obtained on this basis are shown in Figure 4, along with $G_1(f)$, the spectrum of the freely transmitted signal.

The ratio of signal power to non-linear noise power in a slot of width Δf at the bottom of the baseband (corresponding to the worst channel) is then

$$\frac{P_s}{P_n} \approx \frac{[G_1(0)]\,\Delta f}{[G_2(0)+G_3(0)]\,\Delta f} ;$$

and in general, in any channel,

$$\frac{P_s}{P_n} \geq \frac{\alpha^2 W_0}{4\beta^2 BW_0^2 + 18\gamma^2 B^2 W_0^3} .$$

From the definition of the input spectral density

$$W_0 = \frac{\overline{x^2}}{2B} ,$$

we have

$$\frac{P_s}{P_n} \geq \frac{\alpha^2}{2\beta^2\,\overline{x^2} + \frac{9}{2}\gamma^2\left(\overline{x^2}\right)^2} .$$

Note that the signal-to-noise power ratio is given only in terms of the power series coefficients squared and the variance of the Gaussian input.

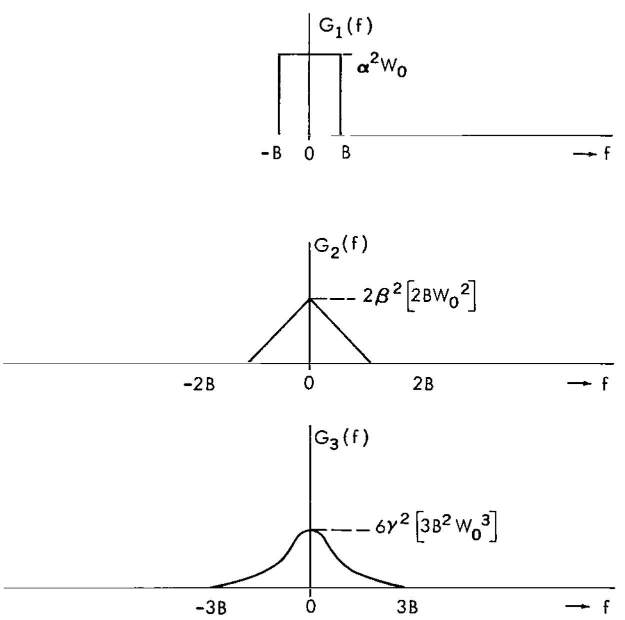

Figure 4—The baseband output spectra $G_1(f)$, $G_2(f)$, and $G_3(f)$.

IF Case

The spectrum of the multichannel signal at IF is shown in Figure 3(b).

The convolutions $S_x(f)*S_x(f)$ and $S_x(f)*S_x(f)*S_x(f)$ for the IF case are evaluated in Appendix C and shown in Figures C10 and C11. The IF output non-linear noise spectra $G_2(f)$ and $G_3(f)$ obtained on this basis are shown in Figure 5, along with $G_1(f)$, the spectrum of the freely transmitted signal. It is immediately clear that for the IF case, all of $G_2(f)$ and the portion of $G_3(f)$ centered at $\pm 3f_0$ fall outside the region of the spectrum occupied by $G_1(f)$, and hence may be assumed to be filtered out by system bandwidth limitations. The portion of $G_3(f)$ centered at $\pm f_0$ is the spectrum of non-linear noise that cannot be filtered out.

The ratio of signal power to noise power in a slot of width Δf at f_0 (corresponding to the worst channel) is

$$\frac{P_s}{P_n} \approx \frac{\left[G_1(f_0)\right] \Delta f}{\left[G_3(f_0)\right] \Delta f} \quad ;$$

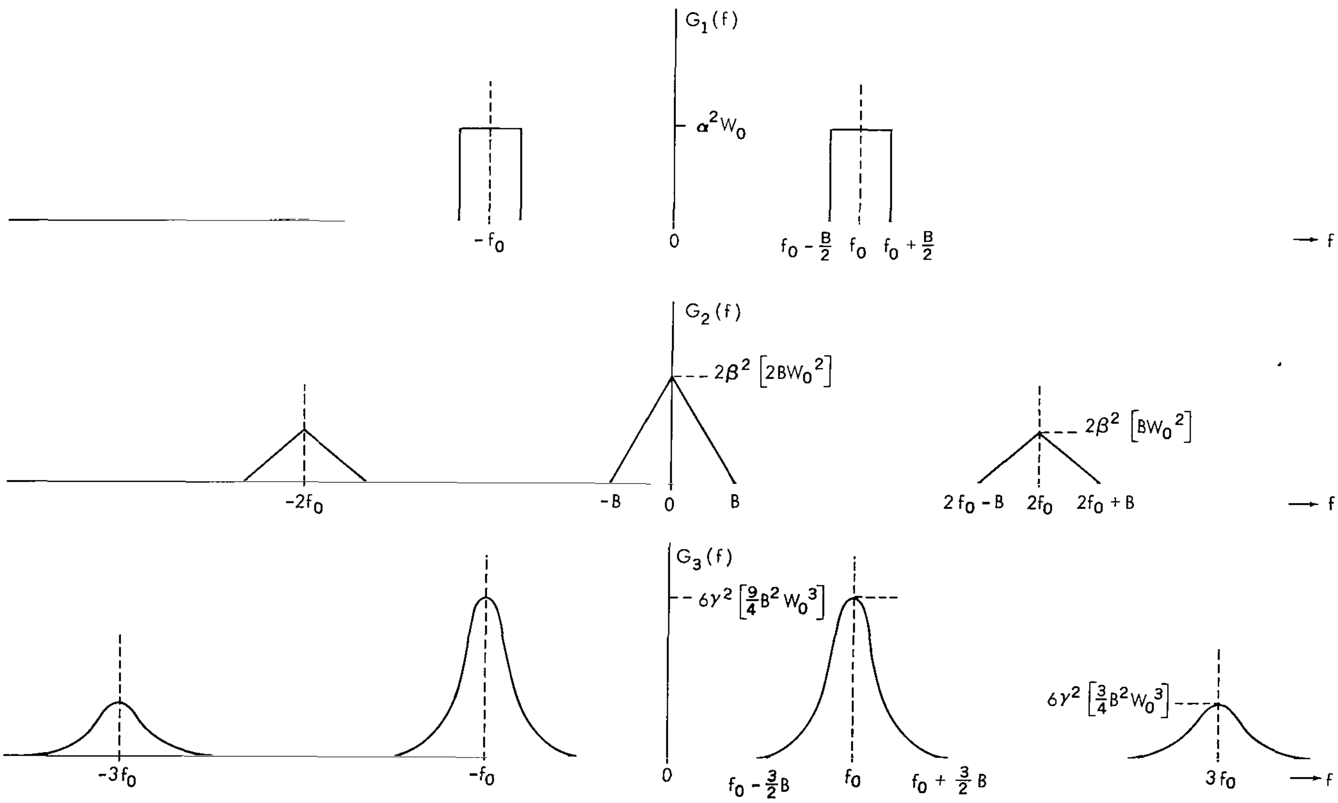

Figure 5—The IF output spectra $G_1(f)$, $G_2(f)$, and $G_3(f)$.

and in any channel

$$\frac{P_s}{P_n} \geq \frac{\alpha^2 W_0}{6\delta^2\left[\frac{9}{4} B^2 W_0^3\right]} .$$

From the definition of W_0,

$$\frac{P_s}{P_n} \geq \frac{8}{27}\left(\frac{\alpha}{\gamma}\right)^2 \frac{1}{\left(\overline{x^2}\right)^2} .$$

Again, the signal to noise power ratio is in terms of the squares of the power series coefficients and the variance of the Gaussian input.

APPLICATION TO ADVANCED SYNCOM

The formulas developed above are directly applicable to certain elements of the SSB-PM FDM telephony mode of the proposed advanced Syncom communication satellite system.

The result for the baseband case

$$\frac{P_s}{P_n} \geq \frac{\alpha^2}{2\beta^2 \overline{x^2} + \frac{9}{2} \gamma^2 \left(\overline{x^2}\right)^2}$$

applies to baseband amplifiers at the ground transmitter and ground receiver, and also the spacecraft modulator* and ground receiver phase demodulator.

The result for the IF case,

$$\frac{P_s}{P_n} \geq \frac{8}{27}\left(\frac{\alpha}{\gamma}\right)^2 \frac{1}{\left(\overline{x^2}\right)^2} ,$$

applies to the SSB exciter chain and power amplifier of the ground transmitter, and the front-end and IF amplifier of the spacecraft receiver.

These signal-to-noise power ratios are analytical equivalents of the "noise-to-noise" power ratio (NPR) measured in a noise loading test as described by White and Whyte, (Reference 3). Since it is customary to characterize the performance of international telephone circuits in terms of a channel test-tone to psophometrically-weighted-noise power ratio, it is necessary to convert the formulas developed above into this form. This is readily done by applying the appropriate CCIR loading factor and NPR conversion factor as discussed in Appendix D.

*It should be pointed out that the phase modulator proposed for the advanced Syncom is unique in that it effectively performs a down-conversion of the multichannel signal in the modulation process. The input to the modulator is at IF, but the phase spectrum of the modulated carrier is at baseband, and demodulation of the carrier yields the multichannel signal at baseband, not at IF.

To illustrate, we consider the linearity requirements of a SSB ground power amplifier for 600 channels. We use the formula for the IF case, and interpret $\overline{x^2}$ as the mean multichannel signal power dissipated through unit resistance into the amplifier:

$$\frac{P_s}{P_n} \geq \frac{8}{27}\left(\frac{\alpha}{\gamma}\right)^2 \frac{1}{\left(\overline{x^2}\right)^2} .$$

The NPR conversion factor for 600 channels is 19.2 db, meaning that the noise-to-noise ratio in a 3.1 kc slot measured in a noise loading test or calculated analytically is 19.2 db poorer than the corresponding channel test-tone to psophometrically-weighted-noise power ratio:

$$\left.\frac{P_{tt}}{P_n}\right|_{\substack{3.1\ \mathrm{kc} \\ \mathrm{weighted}}} \geq \left(10^{1.92}\right) \frac{8}{27}\left(\frac{\alpha}{\gamma}\right)^2 \frac{1}{\left(\overline{x^2}\right)^2} .$$

The loading factor of 600 channels is 12.8 $\mathrm{dbm_0}$, meaning that the mean multichannel signal power is 12.8 db above the power of a channel test-tone:

$$\left.\frac{P_{tt}}{P_n}\right|_{\substack{3.1\ \mathrm{kc} \\ \mathrm{weighted}}} \geq \left(10^{1.92}\right) \frac{8}{27}\left(\frac{\alpha}{\gamma}\right)^2 \frac{1}{\left(10^{1.28}\, P_{tt}\right)^2}$$

$$\geq 10^{-.64} \left(\frac{8}{27}\right)\left(\frac{\alpha}{\gamma}\right)^2 \left(P_{tt}^2\right)^{-1} .$$

This result now specifies how hard the power amplifier may be driven in terms of its power series coefficients; and conversely, for a given power level and allowable non-linear noise level, the permissable ratio of the power series coefficients is specified.

As a second illustration, we consider the linearity requirements of a ground receiver phase demodulator for 1200 channels. We use the formula for the baseband case and interpret $\overline{x^2}$ as the mean square phase deviation $\overline{\phi^2}$ of the modulated carrier into the demodulator:

$$\frac{P_s}{P_n} \geq \frac{\alpha^2}{2\beta^2\, \overline{x^2} + \frac{9}{2}\gamma^2 \left(\overline{x^2}\right)^2} .$$

The NPR conversion factor for 1200 channels is 19.3 db, and the loading factor is 15.8 $\mathrm{dbm_0}$.

$$\left.\frac{P_{tt}}{P_n}\right|_{\substack{3.1\ \mathrm{kc} \\ \mathrm{weighted}}} \geq \frac{\left(10^{1.93}\right) \alpha^2}{2\beta^2\left(10^{1.58}\, \overline{\phi_{tt}^2}\right) + \frac{9}{2}\gamma^2\left(10^{1.58}\, \overline{\phi_{tt}^2}\right)^2}$$

$$\geq 10^{0.35}\, \alpha^2 \left[2\beta^2\, \overline{\phi_{tt}^2} + \frac{9}{2}\gamma^2\, 10^{1.58}\left(\overline{\phi_{tt}^2}\right)^2\right]^{-1} .$$

Again, this result relates the allowable non-linear level in the worst channel to the power series coefficients and the level (in this case, mean-square phase deviation) of the standard channel test-tone.

It should be noted that the results developed here are for a single non-linear element in the SSB-PM system. Non-linear noise accumulates as the signal progresses through the system (Reference 5) and the noise from different elements tends to add up on something between a voltage basis (correlated noise) and a power basis (uncorrelated noise). Worst-case performance can always be calculated by assuming correlation between the non-linear noise sources.

(Manuscript Received September 20, 1963)

REFERENCES

1. Holbrook, B. D., and Dixon, J T., "Load Rating Theory for Multi-Channel Amplifiers," *Bell Syst. Tech. J.* 18:624-644, October 1939 p. 635, fig. 4.

2. Bray, W. J , "The Standardization of International Microwave Radio-Relay Systems," *IEE Proc.* Paper 3412E, 108B:180-200, March 1961 p. 196.

3. White, R. W., and Whyte, J. S., "Equipment for Measurement of Interchannel Crosstalk and Noise on Broadband Multi-Channel Telephone Systems," *Post Off. Elect. Eng. J.* 48(3):127-132, October 1955.

4. Lewin, L., "Interference in Multi-Channel Circuits," *Wireless Eng.* 27:294-304, December 1950.

5. Yeh, L. P., "Consideration of Nonlinear Noise and Its Testing in Frequency Division Multiplex Voice U.H.F. Radio Communication Systems," *IRE Trans. Commun. Syst.* CS-9(2):115-129, June 1961.

Appendix A

Computation of Output Autocorrelation Function

The output is

$$y(t) = \alpha x(t) + \beta x^2(t) + \gamma x^3(t) + \cdots$$

and its autocorrelation function is

$$R_Y(\tau) = \overline{y(t)\, y(t+\tau)} .$$

Truncating the power series, we have

$$y(t)\, y(t+\tau) = \left[\alpha x(t) + \beta x^2(t) + \gamma x^3(t)\right] \cdot \left[\alpha x(t+\tau) + \beta x^2(t+\tau) + \gamma x^3(t+\tau)\right]$$

Carrying out the indicated multiplication,

$$\begin{aligned} y(t)\, y(t+\tau) = {} & \alpha^2 x(t)\, x(t+\tau) + \alpha\beta x(t)\, x^2(t+\tau) + \alpha\gamma x(t)\, x^3(t+\tau) \\ & + \beta\alpha x^2(t)\, x(t+\tau) + \beta^2 x^2(t)\, x^2(t+\tau) + \beta\gamma x^2(t)\, x^3(t+\tau) \\ & + \gamma\alpha x^3(t)\, x(t+\tau) + \gamma\beta x^3(t)\, x^2(t+\tau) + \gamma^2 x^3(t)\, x^3(t+\tau) . \end{aligned}$$

The autocorrelation function is the sum of the expectations of each of these terms.

Middleton* gives a formula for the expectation of the product of Gaussian variables which is directly applicable since $x(t)$ is Gaussian of zero mean and variance $\overline{x^2}$.

$$\text{(a)} \qquad \overline{x^{2N}} = \overline{x_1\, x_2 \cdots x_{2N}} = \sum_{\substack{\text{ALL} \\ \text{PAIRS}}} \left(\prod_{j \neq k}^{N} \overline{x_j\, x_k} \right)$$

$$\text{(b)} \qquad \overline{x^{2N+1}} = 0$$

where N is a positive integer. Formula (b) is intuitively obvious, since

$$\overline{x} = 0$$

*Middleton, D., "An Introduction to Statistical Communication Theory," New York: McGraw-Hill Book Company, 1960 p. 343, eq. 7.28.

and

$$\overline{x^{2N+1}} = \overline{x\left(x^{2N}\right)}$$

Adopting the notation

$$\phi = x(t)\,,$$

$$\theta = x(t+\tau)\,,$$

so that $R_x(\tau) = \overline{\phi\theta}$, and observing that

$$\overline{x^2(t)} = \overline{x^2(t+\tau)} = \overline{\phi^2} = \overline{\theta^2}\,,$$

we note that $\overline{\phi^M \theta^N} = 0$ when $M+N$ = an odd integer. This immediately does away with several of the terms of $R_y(\tau)$. Those which exist are

$$\begin{aligned} R_y(\tau) = {} & \alpha^2\overline{\phi\theta} \\ & + \alpha\gamma\overline{\phi\theta^3} + \alpha\gamma\overline{\phi^3\theta} \\ & + \beta^2\overline{\phi^2\theta^2} \\ & + \gamma^2\overline{\phi^3\theta^3} \end{aligned}$$

Clearly, the first term is identically $\alpha^2 R_x(\tau)$. The other terms can be written out in terms of $\overline{x^2}$ and $R_x(\tau)$.

The other expansions will be worked through completely, following Middleton:

$$\begin{aligned} \overline{\phi\theta^3} &= \overline{\phi\theta_1\theta_2\theta_3} = \overline{\phi\theta_1}\cdot\overline{\theta_2\theta_3} + \overline{\phi\theta_2}\cdot\overline{\theta_1\theta_3} + \overline{\phi\theta_3}\cdot\overline{\theta_1\theta_2} \\ &= 3\overline{\theta^2}\cdot\overline{\phi\theta} = 3\overline{x^2}R_x(\tau)\,; \end{aligned}$$

$$\begin{aligned} \overline{\phi^3\theta} &= \overline{\phi_1\phi_2\phi_3\theta} = \overline{\phi_1\phi_2}\cdot\overline{\phi_3\theta} + \overline{\phi_1\phi_3}\cdot\overline{\phi_2\theta} + \overline{\phi_1\theta}\cdot\overline{\phi_2\phi_3} \\ &= 3\overline{\phi^2}\cdot\overline{\phi\theta} = 3\overline{x^2}R_x(\tau)\,; \end{aligned}$$

$$\begin{aligned} \overline{\phi^2\theta^2} &= \overline{\phi_1\phi_2\theta_1\theta_2} = \overline{\phi_1\phi_2}\cdot\overline{\theta_1\theta_2} + \overline{\phi_1\theta_1}\cdot\overline{\phi_2\theta_2} + \overline{\phi_1\theta_2}\cdot\overline{\phi_2\theta_1} \\ &= \overline{\phi^2}\cdot\overline{\theta^2} + 2\overline{\phi\theta}\cdot\overline{\phi\theta} = \left(\overline{x^2}\right)^2 + 2R_x^2(\tau)\,; \end{aligned}$$

$$
\begin{aligned}
\overline{\phi^3 \theta^3} &= \phi_1 \phi_2 \phi_3 \overline{\theta_1 \theta_2 \theta_3} \\
&= \overline{\phi_1 \phi_2} \cdot \overline{\phi_3 \theta_1 \theta_2 \theta_3} + \overline{\phi_1 \phi_3} \cdot \overline{\phi_2 \theta_1 \theta_2 \theta_3} \\
&\quad + \overline{\phi_1 \theta_1} \cdot \phi_2 \overline{\theta_2 \theta_3 \phi_3} + \overline{\phi_1 \theta_2} \cdot \overline{\phi_2 \phi_3 \theta_1 \theta_3} \\
&\quad + \overline{\phi_1 \theta_3} \cdot \phi_2 \overline{\phi_3 \theta_1 \theta_2} \\
&= \overline{\phi^2} \left[3\overline{\theta^2} \cdot \overline{\phi\theta}\right] + \overline{\phi^2} \left[3\overline{\theta^2} \cdot \overline{\phi\theta}\right] \\
&\quad + \overline{\phi\theta}\left[\overline{\phi^2} \cdot \overline{\theta^2} + 2\overline{\phi\theta} \cdot \overline{\phi\theta}\right] + \overline{\phi\theta}\left[\overline{\phi^2 \theta^2} + 2\overline{\phi\theta} \cdot \overline{\phi\theta}\right] \\
&\quad + \overline{\phi\theta}\left[\overline{\phi^2 \cdot \theta^2} + 2\overline{\phi\theta} \cdot \overline{\phi\theta}\right] \\
&= 9\overline{\phi^2} \cdot \overline{\theta^2} \cdot \overline{\phi\theta} + 6(\overline{\phi\theta})^3 \\
&= 9\left(\overline{x^2}\right)^2 R_x(\tau) + 6R_x^3(\tau) \ ;
\end{aligned}
$$

Thus, finally,

$$
\begin{aligned}
R_y(\tau) &= \beta^2 \overline{x^2} \\
&\quad + \left[\alpha^2 + 6\alpha\gamma\overline{x^2} + 9\gamma^2 \left(\overline{x^2}\right)^2\right] R_x(\tau) \\
&\quad + \left[2\beta^2\right] R_x^2(\tau) \\
&\quad + \left[6\gamma^2\right] R_x^3(\tau) \ .
\end{aligned}
$$

This is the complete expression for the autocorrelation function $R_y(\tau)$ of the output of a non-linear device with a third order power series representation and a Gaussian input of zero mean and variance $\overline{x^2}$.

The output spectrum is the Fourier transform of $R_y(\tau)$:

$$
G_y(f) = \mathfrak{F}\left[R_y(\tau)\right] = \int_{\infty}^{\infty} R_y(\tau)\, e^{-j\omega\tau}\, d\tau
$$

Appendix B

Determination of Power Series Coefficients

The coefficients α, β, γ, etc., of the power series representation of the non-linear device may be determined either analytically or experimentally in a number of ways. For the case of the IF spectra, where the ratio γ/α determines the non-linear noise, there are two simple ways to get γ/α experimentally.

Harmonic Margin Measurement (small signal case)

If the input to the non-linear device is a single tone

$$x(t) = V \cos \omega t$$

the output $y(t)$ will contain harmonics with relative amplitudes which can be readily determined by a wave analyzer:

$$y(t) = A_1 \cos \omega t + A_2 \cos 2\omega t + A_3 \cos 3\omega t + \cdots$$

The harmonic margins A_2/A_1 and A_3/A_1 can be used to evaluate the relative values of α, β, and γ. We have, generally,

$$\begin{aligned} y(t) &= \alpha x(t) + \beta x^2(t) + \gamma x^3(t) + \cdots \\ &= \alpha V \cos \omega t + \beta V^2 \cos^2 \omega t + \gamma V^3 \cos^3 \omega t \\ &= \alpha V \cos \omega t + \beta V^2 \left[\frac{1}{2} + \frac{1}{2} \cos 2\omega t\right] + \gamma V^3 \left[\frac{3}{4} \cos \omega t + \frac{1}{4} \cos 3\omega t\right] + \cdots \end{aligned}$$

or, combining terms and dropping the dc contribution,

$$y(t) = \left[\alpha + \frac{3\gamma V^2}{4}\right] V \cos \omega t + \frac{BV^2}{2} \cos 2\omega t + \frac{\gamma V^3}{4} \cos 3\omega t + \cdots .$$

If $V \ll 1$ (small signal case),

$$y(t) \approx \alpha V \cos \omega t + \frac{BV^2}{2} \cos 2\omega t + \frac{\gamma V^3}{4} \cos 3\omega t + \cdots$$

and the harmonic margins are

$$\left|\frac{A_2}{A_1}\right| = \frac{V}{2}\left|\frac{\beta}{\alpha}\right| ,$$

$$\left|\frac{A_3}{A_1}\right| = \frac{V^2}{4}\left|\frac{\gamma}{\alpha}\right| ;$$

or conversely

$$\left|\frac{\beta}{\alpha}\right| = \frac{2}{V}\left|\frac{A_2}{A_1}\right| ,$$

$$\left|\frac{\gamma}{\alpha}\right| = \frac{4}{V^2}\left|\frac{A_3}{A_1}\right| .$$

Gain Variation Measurement (large signal case)

Using the same expression as above,

$$y(t) = \left[\alpha + \frac{3\gamma V^2}{4}\right] V \cos \omega t + \frac{\beta V^2}{2} \cos 2\omega t$$

$$+ \frac{\gamma V^3}{4} \cos 3\omega t + \cdots .$$

assuming harmonic terms are filtered out, and removing restrictions on the magnitude of V, we have that

$$\frac{y(t)}{x(t)} = \alpha + \frac{3\gamma V^2}{4} = \alpha\left[1 + 3\,\frac{\gamma}{\alpha}\,\frac{V^2}{4}\right] ,$$

where the normalized gain is defined as

$$G = \frac{y(t)}{\alpha x(t)} .$$

If the magnitude of the input signal is varied by ΔV, there is a change in gain

$$\Delta G = \frac{3}{4}\left(\frac{\gamma}{\alpha}\right)(\Delta V)^2 .$$

Under certain conditions this is an excellent way to measure the ratio γ/α . This ratio may be either positive or negative in sign; e.g., for a limiting amplifier, the sign would be negative.

Appendix C

Evaluation of Spectral Convolutions

To evaluate the Fourier transform of the output autocorrelation function as computed in Appendix A, we must compute the transforms

$$F(f) = \mathcal{F}\left[R_x^2(\tau)\right] = \int_{-\infty}^{\infty} R_x^2(\tau)\, e^{-j\omega\tau}\, d\tau$$

and

$$H(f) = \mathcal{F}\left[R_x^3(\tau)\right] = \int_{-\infty}^{\infty} R_x^3(\tau)\, e^{-j\omega\tau}\, d\tau\ ,$$

where $R_x(\tau)$ is given by

$$R_x(\tau) = \int_{-\infty}^{\infty} S_x(f)\, e^{j\omega\tau}\, df = \overline{x(t)\, x(t+\tau)}\ ,$$

$$R_x(0) = \int_{-\infty}^{\infty} S_x(f)\, df = \overline{x^2(t)}\ .$$

We have that

$$F(f) = \int_{-\infty}^{\infty} R_x^2(\tau)\, e^{-j\omega\tau}\, d\tau = \int_{-\infty}^{\infty} R_x(\tau) \left[\int_{-\infty}^{\infty} S_x(f)\, e^{j\omega\tau}\, df\right] e^{-j\omega\tau}\, d\tau$$

or, more concisely, introducing a new dummy variable λ to avoid confusion,

$$F(f) = \int_{-\infty}^{\infty} \int_{-\infty}^{\infty} R_x(\tau)\, S_x(\lambda)\, e^{j2\pi\lambda\tau}\, e^{-j\omega\tau}\, d\lambda\, d\tau$$

$$= \int_{-\infty}^{\infty} \int_{-\infty}^{\infty} R_x(\tau)\, S_x(\lambda)\, e^{-j(\omega-2\pi\lambda)\tau}\, d\lambda\, d\tau\ ;$$

$$S_x(f-\lambda) = \int_{-\infty}^{\infty} R_x(\tau)\, e^{-j(\omega-2\pi\lambda)\tau}\, d\tau\ ;$$

$$F(f) = \int_{-\infty}^{\infty} S_x(\lambda)\, S_x(f-\lambda)\, d\lambda = S_x(f) * S_x(f)$$

This result is known as the Borel or convolution theorem. Similarly,

$$H(f) = \int_{-\infty}^{\infty} S_x(\theta)\, d\theta \int_{-\infty}^{\infty} S_x(\lambda)\, S_x(f-\lambda)\, d\lambda$$

$$= S_x(f) * S_x(f) * S_x(f)$$

It is required to compute $S_x(f)*S_x(f)$ and $S_x(f)*S_x(f)*S_x(f)$ for baseband and IF input spectra as shown below in Figures C1 and C2.

To do this, we start with the baseband spectrum (which we now designate $S_L(f)$, and compute $S_L(f)*S_L(f)$ and $S_L(f)*S_L(f)*S_L(f)$. These results are then used to get the results for the IF spectrum.

To get $S_L(\lambda - f)$, $S_L(f)$ is displaced to the left (for positive λ) and then folded about the point $f = 0$ (Figure C3).

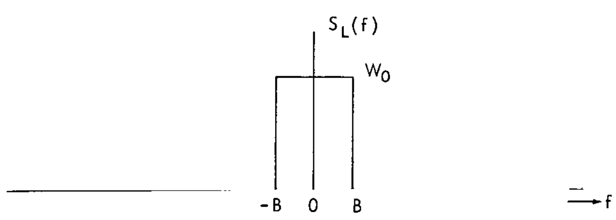

Figure C1—The input baseband spectrum $S_L(f)$.

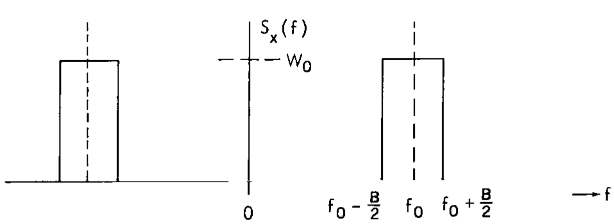

Figure C2—The input IF spectrum $S_x(f)$.

For values of displacement less than $-2B$, there is no overlap and the convolution is zero. At $\lambda = -2B$, the displaced function starts to overlap $S_L(f)$, and the convolution has a value

$$S_L(f)*S_L(f) = \int_{-B}^{B+\lambda} (W_0)(W_0)\, df = W_0^2\,(2B+\lambda) .$$

This expression holds for values of displacement

$$-2B < \lambda < 0 .$$

For positive values of displacement, the limits of the integral must be changed, and the convolution (Figure C4) is

$$S_L(f)*S_L(f) = \int_{-B+\lambda}^{B} W_0^2\, df = W_0^2\,(2B-\lambda) .$$

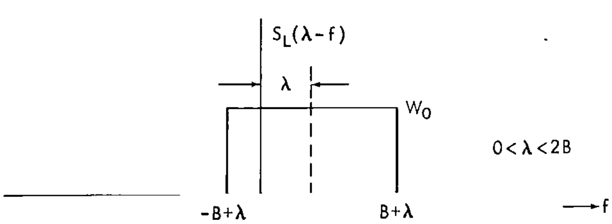

Figure C3—The spectrum $S_L(\lambda - f)$ for a small positive displacement λ.

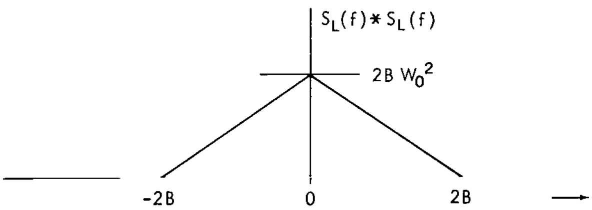

Figure C4—The spectrum of the convolution $S_L(f)*S_L(f)$.

The abscissa is frequency, which we label f (instead of λ), and the ordinate is spectral density. Note that the symmetry of $S_L(f)$ produces a convolution which is an even function of frequency.

To evaluate the iterated convolution $S_L(f)*S_L(f)*S_L(f)$, the piecewise technique described by Lee* is used. The convolution $S_L(f)*S_L(f)$ as computed above is broken into two auxiliary functions g(f) and h(f), each is convolved separately with $S_L(f)$, and the results are superposed. In Figure C5 (a through g) the auxiliary functions g(f) and h(f) are shown, and three conditions of displacement of $S_L(\lambda - f)$ are shown. The "boxcar" slides from left to right as λ goes from $-\infty$ to ∞.

By careful inspection, it is observed that the convolution of $S_L(f)$ with g(f) is given by

$$g(f)*S_L(f) = I_1 + I_2$$

where

$$I_1 = \int_{-2B}^{\lambda+B} (W_0)(W_0^2)(f + 2B)\,df\ , \quad -3B \le \lambda \le -B,$$

and

$$I_2 = \int_{\lambda-B}^{0} (W_0)(W_0^2)(f + 2B)\,df\ , \quad -B \le \lambda \le B;$$

and is zero for values of displacement

$$-B > \lambda$$

and

$$3B < \lambda\ .$$

*Lee, Y. W., "Statistical Theory of Communication," New York: John Wiley & Sons, 1960 p. 24.

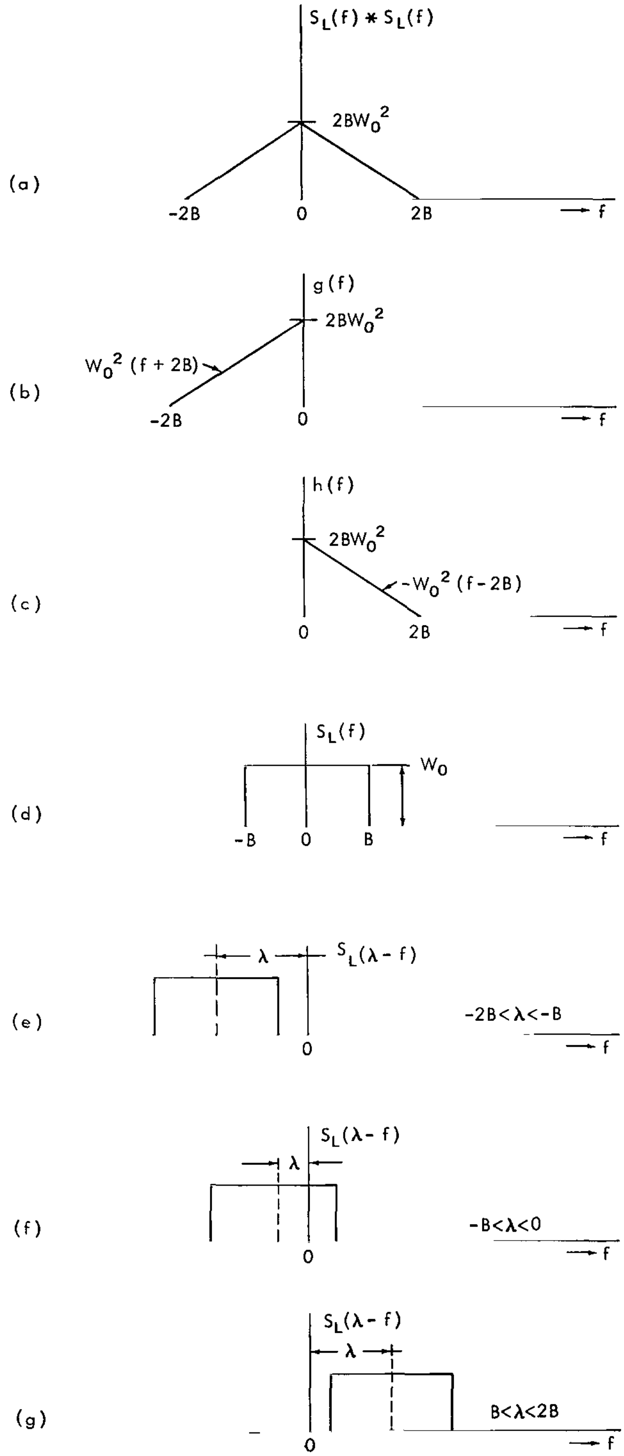

Figure C5—The auxiliary functions g(f) and h(f), and three conditions of displacement of $S_L(\lambda - f)$.

Likewise, we have that the convolution of $h(f)$ with $S_L(f)$ is given by

$$h(f) * S_L(f) = I_3 + I_4$$

where

$$I_3 = -\int_0^{\lambda+B} \left(W_0\right)\left(W_0^2\right) (f - 2B)\, df\,, \qquad -B \leq \lambda \leq B,$$

$$I_4 = -\int_{\lambda-B}^{2B} \left(W_0\right)\left(W_0^2\right) (f - 2B)\, df\,, \qquad B \leq \lambda \leq 3B;$$

and is zero for values of displacement

$$-B > \lambda$$

$$3B < \lambda\,.$$

The iterated convolution is then

$$S_L(f) * S_L(f) * S_L(f) = I_1 + I_2 + I_3 + I_4\,.$$

Particular attention must be paid to the exact domain of definition of each of the integrals.

The four integrals are evaluated, graphed, and superposed to yield the result. The first two are

$$I_1 = \int_{-2B}^{\lambda+B} W_0^3 (f + 2B)\, df = W_0^3 \left[\frac{f^2}{2} + 2Bf\right]_{-2B}^{\lambda+B};$$

$$I_1 = \frac{1}{2} W_0^3 \left[9B^2 + 6B\lambda + \lambda^2\right], \qquad -3B \leq \lambda \leq -B\,;$$

$$I_2 = \int_{\lambda-B}^{0} W_0^3 (f + 2B)\, df = W_0^3 \left[\frac{f^2}{2} + 2Bf\right]_{\lambda-B}^{0};$$

$$I_2 = \frac{1}{2} W_0^3 \left[3B^2 - 2B\lambda - \lambda^2\right], \qquad -B \leq \lambda \leq B\,;$$

in which we note that

$$I_1(-3B) = I_2(B) = 0\,,$$

$$I_1(-B) = I_2(-B) = 2B^2 W_0^3\,,$$

$$I_2(0) = \frac{3}{2} B^2 W_0^3\,.$$

and the second two integrals are

$$I_3 = -\int_0^{\lambda+B} W_0^2\,(f - 2B)\,df = W_0^3\left[\frac{f^2}{2} - 2Bf\right]_0^{\lambda+B} ;$$

$$I_3 = -\frac{1}{2}\,W_0^3\left[-3B^2 - 2B\lambda + \lambda^2\right] , \qquad -B \le \lambda \le B ;$$

$$I_4 = -\int_{\lambda-B}^{2B} W_0^3\,(f - 2B)\,df = W_0^3\left[\frac{f^2}{2} - 2Bf\right]_{\lambda-B}^{2B} ;$$

$$I_4 = -\frac{1}{2}\,W_0^3\left[-9B^2 + 6B\lambda - \lambda^2\right] , \qquad B \le \lambda \le 3B ;$$

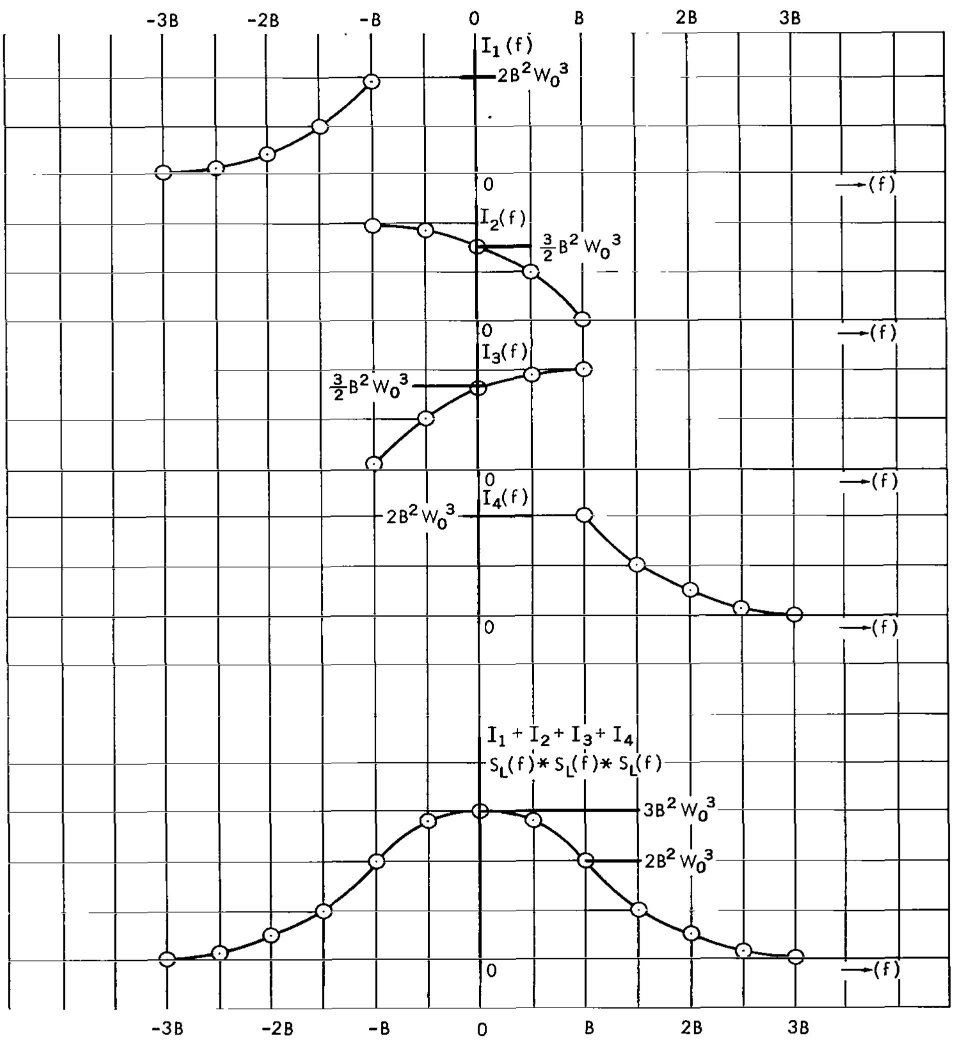

Figure C6—Superposition of I_1, I_2, I_3, and I_4 to give the iterated convolution $S_L(f) * S_L(f) * S_L(f)$.

in which we note that

$$I_3(-B) = I_4(3B) = 0 ,$$

$$I_3(B) = I_4(B) = 2B^2 W_0^3 ,$$

$$I_3(0) = \frac{3}{2} B^2 W_0^3 .$$

The superposition of the four integrals to give the iterated convolution $S_L(f) * S_L(f) * S_L(f)$ is shown in Figure C6.

Using these results, we can now evaluate the result for the IF spectrum by inspection. The calculated convolutions are shown in Figure C7. Auxiliary convolutions in slightly different notation can be derived by inspection and are shown in Figure C8.

The IF spectra $S_x(f)$ and $S_x(\lambda - f)$ are shown in Figure C9. As λ increases from $-\infty$, boxcar IV will overlap boxcar I as $\lambda \to -2f_0$ generating a triangular spectrum (Figure C8-b).

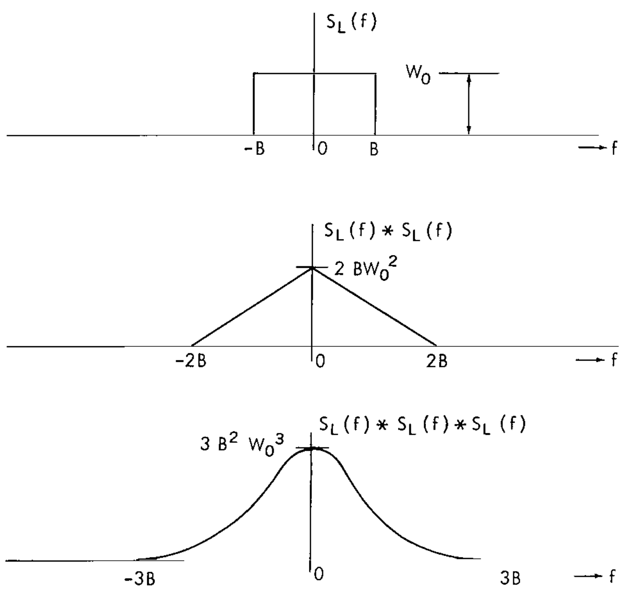

Figure C7—The spectra of the convolutions $S_L(f)$, $S_L(f) * S_L(f)$, and $S_L(f) * S_L(f) * S_L(f)$.

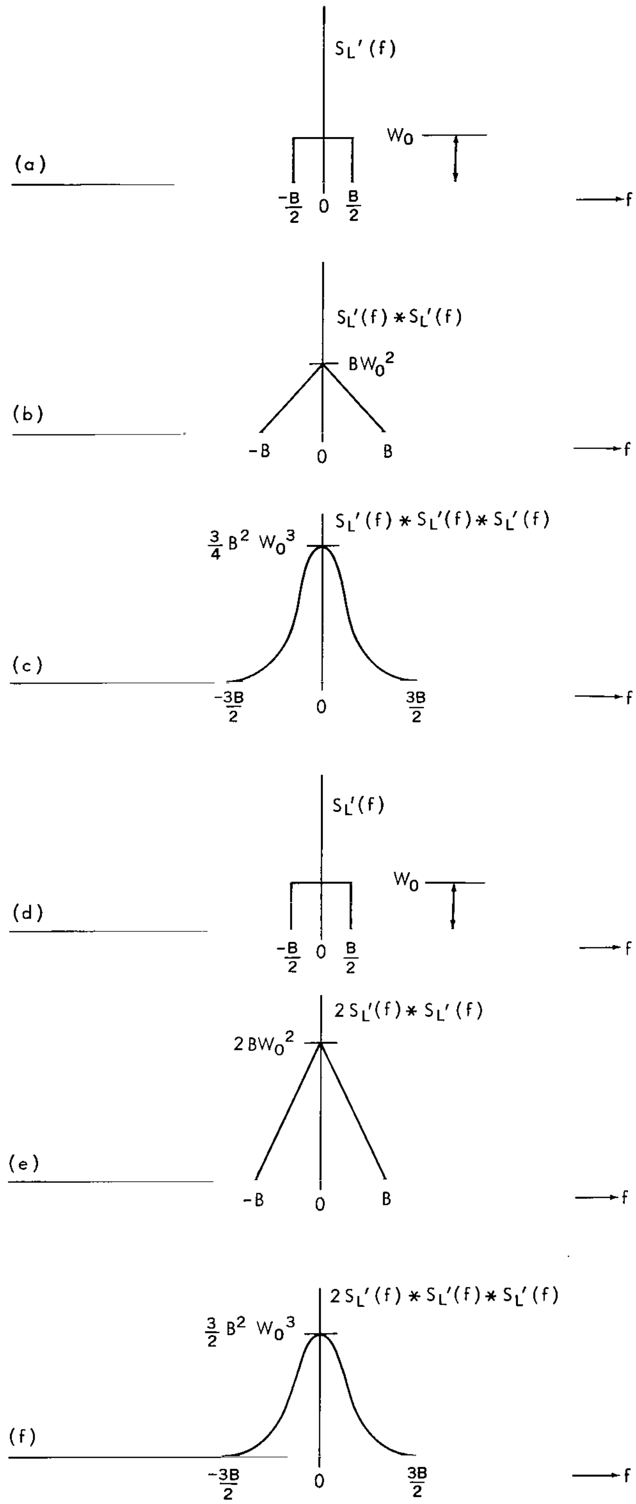

Figure C8—Auxiliary convolutions.

As the displacement nears zero, boxcars III and IV will overlap boxcars I and II, respectively, at the same time, generating a triangular spectrum centered at zero frequency (Figure C8-e). As λ increases positively, a triangular spectrum (Figure C8-b) is generated at $\lambda = 2f_0$, and the spectrum of the convolution is shown in Figure C10.

If we now convolve this second order spectrum with $S_x(f)$, we see that as λ increases from $-\infty$ and nears $-3f_0$, boxcar IV (Figure C9) overlaps triangle V, generating a bell-shaped spectrum (Figure C8-c) at $-3f_0$. As λ increases to $-f_0$, boxcar IV overlaps triangle VI simultaneously as boxcar III overlaps triangle V, generating a bell shaped spectrum (Figure C8-f) at $-f_0$.

For positive λ, a mirror image results, and we have the result shown in Figure C11.

It can be seen that a further convolution of $S_x(f)$ will produce fourth order distortion spectra at 0, $\pm 2f_0$, and $\pm 4f_0$. This is not computed because such spectra may be readily filtered out, as was noted earlier.

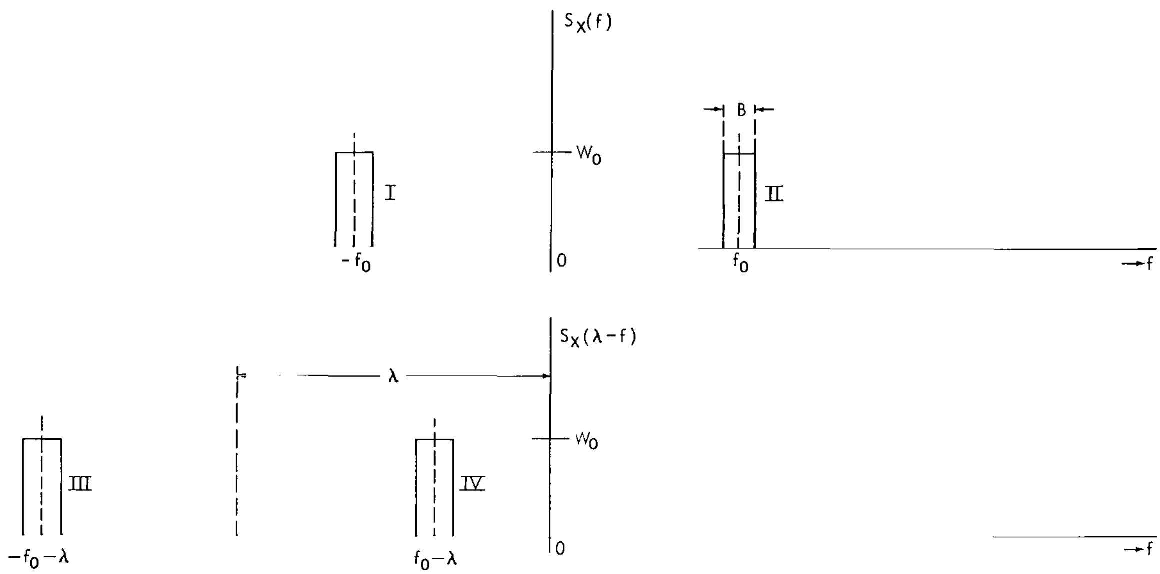

Figure C9—The input IF spectra $S_x(f)$ and $S_x(\lambda - f)$.

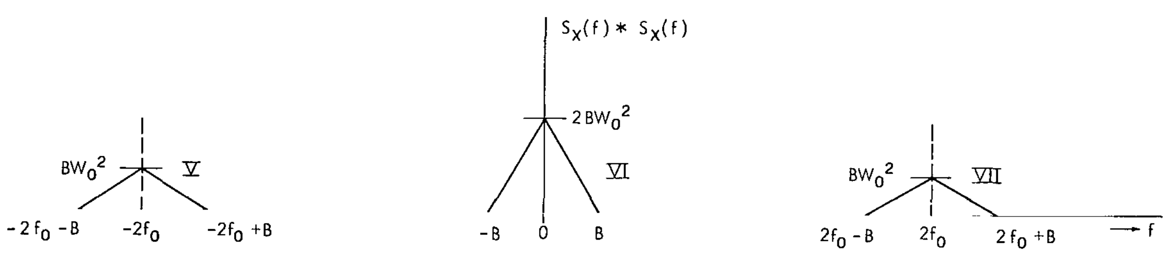

Figure C10—The spectrum of $S_x(f) * S_x(f)$.

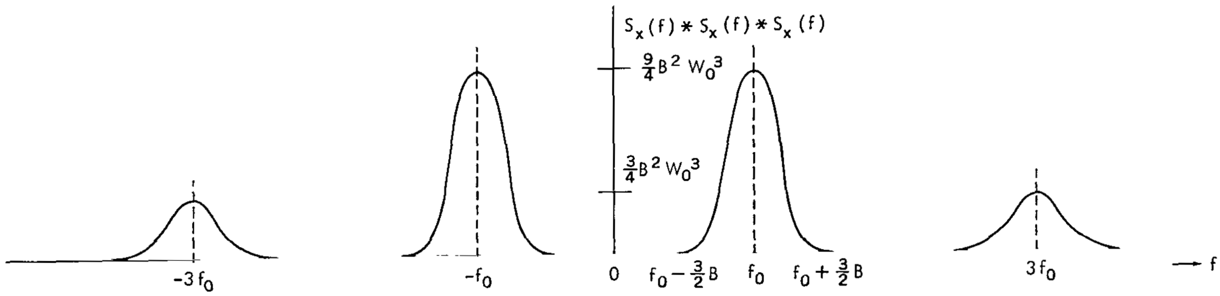

Figure C11—The spectrum of $S_x(f) * S_x(f) * S_x(f)$.

Appendix D

Discussion of Channel Loading Factor, NPR Conversion Factor, and Multichannel Peak Factor

To avoid ambiguity, it is convenient to specify the intensity of a multichannel signal in terms of the power of a single channel test-tone at a point of zero relative level. The CCIR recommends desirable multichannel signal levels and allowable noise levels in dbm_0, or decibels with respect to one milliwatt at zero relative level. The phrase "zero relative level" refers to some physical point in the communication system where channel test-tone level happens to be exactly 1 mw, or 0 dbm_0. The statement that for 1200 channels the multichannel signal is 15 dbm_0 means that at any point in the system, the multichannel signal power is 15 db above the channel test-tone power, and at zero relative level it is exactly 15 dbm_0 or 31.6 milliwatts. The CCIR recommended loading factors for busy-hour traffic are

$$10 \log_{10} \frac{P_s}{P_{tt}} = -1 + 4 \log_{10} N \quad dbm_0 , \qquad 12 \leq N \leq 240 ;$$

and

$$10 \log_{10} \frac{P_s}{P_{tt}} = -15 + 10 \log_{10} N \quad dbm_0 , \qquad N > 240 .$$

These equations are graphed as curves (a) and (b) in Figure D1.

The CCIR noise-power-ratio conversion factor may be regarded as an allowance for the difference between channel test-tone level and the portion of the noise-power loading which is effectively applied to any one channel in a noise-loading test; i.e., for a 1200 channel system, the loading factor is 15.8 dbm_0, and the baseband is 5.6 Mc wide. The noise power falling into a 3.1 kc slot is 3.1/5600 of the applied power or -32.6 db with respect to +15.8 dbm_0; and it is -32.6 +15.8 = -16.8 db with respect to 0 dbm_0, the channel test-tone power at zero relative level. Psophometric filtering reduces the noise by 2.5 db, so the NPR conversion factor for 1200 channels is 16.8 +2.5 or 19.3 db. CCIR NPR conversion factors are given as curves (c) and (d) of Figure D1.

For a single speech channel, peaks as high as 19 db above the rms level are encountered. As many speech channels are multiplexed together, the composite signal peak-to-average ratio falls off, and for more than 800 channels it levels off at about 13 db. Multichannel peak factors from Holbrook and Dixon* are given as curve (e) in Figure D1.

*Holbrook, B. D., and Dixon, J. T., "Load Rating Theory for Multi-Channel Amplifiers," *Bell Syst. Tech J.* 18:624-644, October 1939.

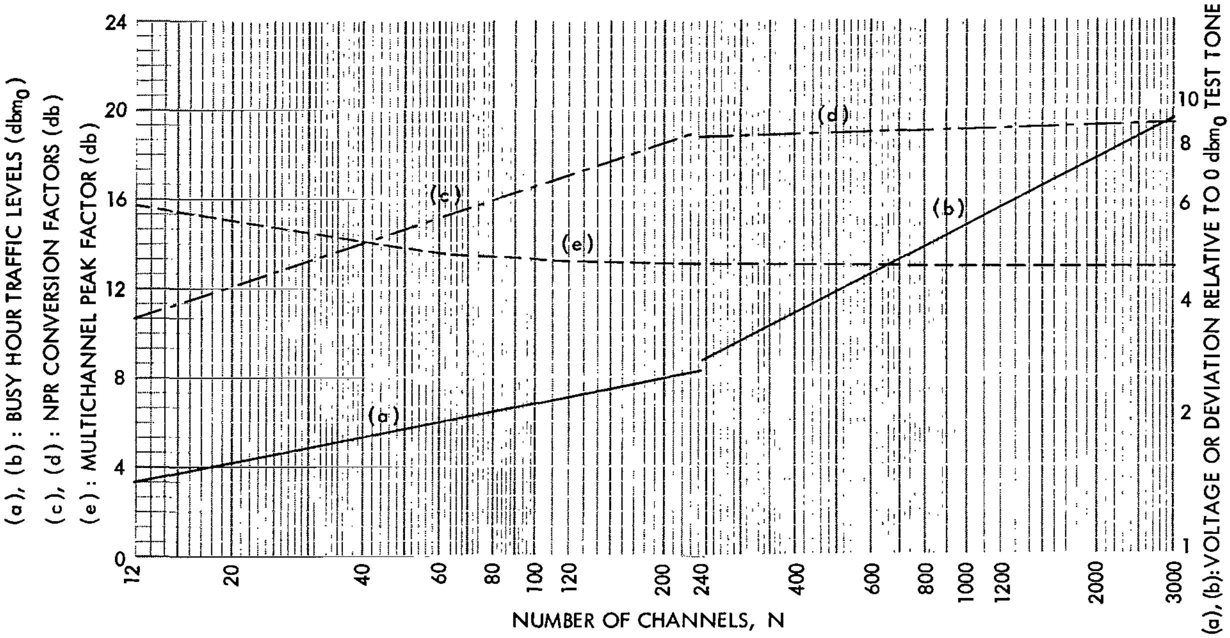

Figure D1—CCIR channel loading factors and conversion factors, and Holbrook-and-Dixon peak factors. The conversion factor is added to the noise power ratio to give the S/N ratio for 1 mw of tone and noise power in a 3.1 kc band, psophometrically weighted. The unweighted noise power in a 3.1 kc band is 2.5 db greater than the psophometrically weighted noise.

NASA-Langley, 1964 G-517